Porous activated carbons derived from waste Moroccan pine cones for high-performance adsorption of bisphenol A from water

Yassine Jari, Nicolas Roche, Mohamed Chaker Necibi, Fatima Zahra Falil, Saida Tayibi, Karim Lyamlouli, Abdelghani Chehbouni, Bouchaib Gourich

Heliyon 10 (2024) e29645

Contents lists available at ScienceDirect

Heliyon

journal homepage: www.cell.com/heliyon

Research article

Porous activated carbons derived from waste Moroccan pine cones for high-performance adsorption of bisphenol A from water

Yassine Jari [a], Nicolas Roche [a,b], Mohamed Chaker Necibi [a], Fatima Zahra Falil [c], Saida Tayibi [d], Karim Lyamlouli [d], Abdelghani Chehbouni [a,e], Bouchaib Gourich [a,c,*]

[a] International Water Research Institute (IWRI), Mohammed VI Polytechnic University, Ben Guerir, 43150, Morocco
[b] Aix-Marseille University, CNRS, IRD, INRAE, Coll France, CEREGE, CEDEX, 13454, Aix-en-Provence, France
[c] Laboratory of Process and Environmental Engineering, Higher School of Technology, Hassan II University of Casablanca, Morocco
[d] AgroBioSciences (AgBS), College of Sustainable Agriculture and Environmental Science (CSAES), Mohammed VI Polytechnic University (UM6P), Benguerir, 43150, Morocco
[e] Centre D'études Spatiales de La Biosphère (Cesbio), Institut de Recherche Pour le Développement (IRD), Unité Mixte de Recherche (UMR), 31401, Toulouse, France

ARTICLE INFO

Keywords:
Porous activated carbon
Pine cones
Adsorption-desorption
Bisphenol A
Regeneration
Water

ABSTRACT

Porous-activated carbons (ACs) derived from Moroccan pine cones (PC) were synthesised by a two step-chemical activation/carbonisation method using phosphoric acid (PC-H) and zinc chloride (PC-Z) as activating agents and used for the adsorption of bisphenol A (BPA) from water. Several techniques (TGA/DTA, FT-IR, XRD, SEM and BET) were used to determine the surface area and pore characterisation and variations during the preparation of the adsorbents. The modification significantly increased the surface area of both ACs, resulting in values of 1369.03 $m^2\ g^{-1}$ and 1018.86 $m^2\ g^{-1}$ for PC-H and PC-Z, respectively. Subsequent adsorption tests were carried out, varying parameters including adsorbent dosage, pH, initial BPA concentration, and contact time. Therefore, the highest adsorption capacity was observed when the BPA molecules were in their neutral form. High pH values were found to be unfavourable for the removal of bisphenol A from water. The results showed that BPA adsorption kinetics and isotherms followed pseudo-second-order and Langmuir models. Thermodynamic studies indicated that the adsorption was spontaneous and endothermic. Besides, the regeneration of spent adsorbents demonstrated their reusability. The adsorption mechanisms can be attributed to physical adsorption, hydrogen bonds, electrostatic forces, hydrophobic interactions, and π-π intermolecular forces.

1. Introduction

Water is an essential ingredient for all living beings, required to sustain life. However, the rapid growth of anthropogenic activities has created unbearable pressure on the environment by generating large amounts of new chemicals called emerging contaminants (ECs) that seriously threaten water quality on a global scale [1]. Thus, water contamination has become a crucial issue in several countries that do not have effective water treatment processes. ECs include endocrine disruptors, pesticides, pharmaceuticals, personal

* Corresponding author. International Water Research Institute (IWRI), Mohammed VI Polytechnic University, Ben Guerir, 43150, Morocco.
E-mail addresses: Yassine.JARI@um6p.ma (Y. Jari), Nicolas.ROCHE@um6p.ma (N. Roche), Chaker.NECIBI@um6p.ma (M. Chaker Necibi), fz.falil@gmail.com (F. Zahra Falil), Saida.TAYIBI@um6p.ma (S. Tayibi), Abdelghani.CHEHBOUNI@um6p.ma (A. Chehbouni), gourichb@gmail.com (B. Gourich).

https://doi.org/10.1016/j.heliyon.2024.e29645
Received 7 December 2023; Received in revised form 16 March 2024; Accepted 11 April 2024
Available online 16 April 2024

care products, flame retardants, polycyclic aromatic hydrocarbons, microplastics, viruses, etc [2,3]. These substances can enter source waters and affect human life and biota ecology, even at very low concentrations (μg-ng L^{-1}) [4]. However, some researchers have investigated their presence in the aquatic environment, including surface water, seawater, groundwater, drinking water, and wastewater [5–7]. According to reported studies, existing conventional wastewater treatment technologies are ineffective in removing this new type of pollutants from wastewater, allowing them to be discharged into receiving water bodies and threatening the sustainability of the ecosystem [8].

Bisphenol A (BPA) is an endocrine-disrupting compound widely used to produce polymeric materials such as polycarbonates and epoxy resins [9]. Exposure to BPA can lead to numerous effects in humans, including ovarian and testicular cancers, diabetes, obesity, hypertension and heart disease [10]. BPA has been detected in various water environments such as groundwater (71.1 ng/L), industrial wastewater (1468.3 ng/L), drinking water (2230 ng/L), surface water (1085.3 ng/L), and seawater (4160–16920 ng/L) [6,11] at trace levels (from ng/L to μg/L) and even in low concentrations it can cause serious damage to humans and aquatic species. Its toxicity and endocrine-disrupting properties have prompted industry and researchers to seek effective methods to remove it from wastewater before its release into the receiving environment [12]. Several treatment techniques have been applied to handle this toxic chemical, including electrocoagulation, advanced oxidation, membrane filtration, biodegradation, and adsorption [13]. Among these, adsorption is regarded as an effective technology for the treatment of various contaminants in water and wastewater streams due to its simplicity, high efficiency, low cost, versatility to remove a wide range of pollutants, and absence of harmful by-products [14]. As well, it can be applied for large scale water and wastewater treatment scenarios.

Carbon-based adsorbents are the most widely used materials for separating and purifying both gaseous and liquid phase mixtures [15]. Unfortunately, the cost of commercial activated carbon is quite expensive, which remains one of the main drawbacks of its use. However, a growing research interest is in developing low-cost, environmentally friendly materials with good pollutant adsorption potential from available sources [16]. The cost involved in the production of the AC using waste as a precursor was pointed out by the authors as quite lower than the price of a commercial AC used for wastewater treatment (DARCO 56€/250 g, Norit PK 52€/250 g, and Norit*SX2 66€/250 g) as referred by Bhomick et al. [17]. In this regard, biomass waste valorisation has become a research hotspot [18]. In recent years, a significant amount of waste materials (such as forestry and agricultural residues, municipal solid waste and industrial by-products), which are abundant in nature, have been successfully used to develop effective materials as a new generation of carbonaceous materials that can replace current adsorbents [19]. These materials are characterised by the high capture capacity of different substances, large surface area, large pore volumes, high micropores, and better adsorption capacity [20,21]. Indeed, biomass-derived AC was intensively investigated from different feedstocks such as wheat straw, palm shell, potato peels, coffee waste, tea Leaves, coconut shell, *Croton caudatus* and *Prosopis juliflora* [15,22–28].

However, the most important challenge is selecting favourable biomass types from a wide range of efficient, green, and sustainable materials. Pine tree is one of the most economical tree species worldwide because of its wood [29]. It is widely available in many areas of Morocco and generates large amounts of pine cones as waste that have not been widely used so far. Indeed, pine cones (PC) are forestry by-products that are present in the environment without being properly used for any purpose and can be converted into value-added materials such as activated carbon. They are mainly composed of hemicelluloses, cellulose, lignin and resins that contain various organic compounds [30]. The possibility of using PC as a raw precursor for the preparation of ACs is very advantageous owing to its abundantly, readily available, economic, and is formed annually in considerable quantities (renewable nature), which makes it a promising and low-cost biomaterial for environmental applications.

Although the literature has reported the synthesis of porous carbon from pine cones and their use for the removal of emerging contaminants, dyes, and metals from aqueous solutions by adsorption, no study has been carried out to date on Moroccan pine cones as a precursor for AC synthesis, nor on the evaluation and comparison of BPA adsorption performance using different activating agents, to the best of our knowledge. Therefore, the present study evaluated the performance of Moroccan pine cones (*Pinus halepensis*) as a natural source for the preparation of activated carbons for removing bisphenol A (BPA) from water using the batch adsorption process. Pine cones were used to produce ACs after chemical activation with H_3PO_4 and $ZnCl_2$ and carbonisation under the same preparation conditions. The schematic preparation process of the adsorbents is illustrated in Fig. 1. The prepared carbon materials were

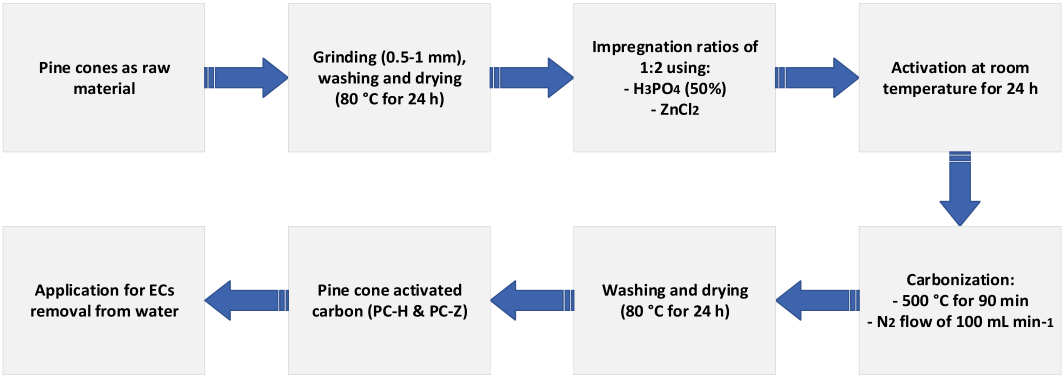

Fig. 1. Schematic preparation process of adsorbents for BPA removal.

characterised using various techniques and comparatively analysed. The influence variables, such as adsorbent dosage, pH, initial BPA concentration and contact time, were investigated. Moreover, the adsorption isotherm, kinetic, thermodynamic, and regeneration of the saturated carbons were analysed.

2. Materials and methods

2.1. Chemicals and reagents

Moroccan pine cones (*Pinus halepensis*) were collected locally from a forest in the province of Sefrou, in the Fez-Meknes region, Morocco. Zinc chloride ($ZnCl_2$), and ortho-phosphoric acid, (H_3PO_4, 85 % w/w.) were purchased from Scharlau (Spain). Bisphenol A (≥99 % purity) was procured from Sigma Aldrich (Germany). Hydrochloric acid (HCl, ≥37 %), and sodium hydroxide (NaOH, ≥97 %) were purchased from Fluka (Germany). Ethanol was supplied by Biosmart (Morocco). Reverse osmosis (RO) water was prepared in the laboratory using an RO purification system (Elettronica Veneta) and used to prepare BPA solutions for adsorption experiments. All reagents were used as received without further purification. Table 1 presents the representative emerging contaminant selected for assessing the performance of the prepared activated carbons for water treatment: bisphenol A (BPA).

2.2. Preparation of activated carbons

Prior to pyrolysis, the pine cones were washed repeatedly with clear water, then with osmosis water to remove dust and impurities and dried at 353 K for 24 h. The cones were ground in a domestic blender and sieved through a 0.5–1 mm sieve. The lab-made activated carbons were prepared by chemical activation of the biomass, using phosphoric acid H_3PO_4 and zinc chloride $ZnCl_2$. In a typical synthesis [17,31,32], 50 g of PC was mixed in a beaker with H_3PO_4 (50 %) or $ZnCl_2$ (100 g of $ZnCl_2$ in 200 ml of osmosis water) solutions with the impregnation ratios of 1:2 of the weight of biomass/impregnation reagent. The mixture was stirred continuously at room temperature for 24 h and then dried at 383 K for 24 h. Next, the impregnated samples were pyrolysed in an electrical furnace (Nabertherm GmbH, Germany) at 773 K under N_2 flow of 100 mL min^{-1} at the heating rate of 283 K min^{-1} from room temperature to 773 K and kept at 773 K for 90 min. After pyrolysis, the furnace was cooled to room temperature in a nitrogen gas stream overnight.

Lastly, the excess activating agents were removed by washing the prepared samples with NaOH (0.1 M) and hot osmosis water until neutral pH and dried at 353 K for 24 h. The activated carbons thus prepared were designated with PC (from pine cones) followed by the letter H (PC-H) for phosphoric acid and Z (PC-Z) for zinc chloride activation.

2.3. Characterisation

PC, PC-H, and PC-Z were characterised using various advanced techniques. Thermogravimetric analysis (TGA/DTA) was performed using LINSEIS STA PT 1600, to determine the raw PC's thermal behaviour from room temperature to 973 K (in air, 283 K). Accordingly, the morphology of materials was analysed on a Hirox SH 4000 M Scanning Electron Microscope (SEM) at 10 kV, the sample surface was scanned at 2500 × and 3500 × magnification ratios. Diffractograms (XRD) were obtained through a D8 ADVANCE (Bruker) diffractometer, in the 2θ range from 10° to 80°, with 40 kV voltage and 40 mA current. Fourier transform infrared spectra were recorded on an FT/IR–4X, JASCO spectrometer in the 400-4000 cm^{-1} range. Specific surface area analysis was determined using Brunauer-Emmett-Teller (BET) method, and pore size distribution was performed using the Barrett-Joyner-Halenda (BJH) method from the nitrogen adsorption-desorption isotherms using a Micromeritics Gemini VII system, USA. Operating at a liquid nitrogen temperature of 77 K. Before these measurements, the samples were degassed at 523 K for 12 h under vacuum.

2.4. Experimental setup

The performance of prepared activated carbons was evaluated and compared towards the adsorption of the BPA through batch adsorption experiments that were conducted in at least triplicate. All experiments were carried out in 250 ml flasks using the initial concentration of 50 mg L^{-1} at 293 K and a constant stirring (180 rpm). One-factor-at-a-time (OFAT) method was applied. Parameters influencing the adsorption process, including adsorbent mass (0.01–0.12 g), pH (2–12), and temperature (293–313 K) were

Table 1
General physicochemical properties of BPA [19].

Properties	Bisphenol A
Molecular Formula	$C_{15}H_{16}O_2$
Chemical structure	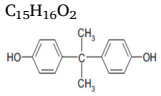
Density ($g.cm^{-3}$)	1.20
Molecular weight ($g.mol^{-1}$)	228.291
Water solubility (mg. L^{-1})	120–300
Dissociation constant, pK_a	10.29

investigated. Otherwise, initial BPA content, pH, and temperature were equal to 50 mg L^{-1}, 6.7, and 293 K, respectively. The different pH solutions were prepared by regulating the initial solution with 0.1 M HCl or NaOH solution as required.

Kinetics experiments were carried out using 100 ml of 50 mg L^{-1} BPA solution with 0.04 g and 0.1 g mass of PC-H and PC-Z, respectively, with time intervals from 15 to 1800 min at 298 K, taking samples at regular time intervals until the adsorption equilibrium was reached. Adsorption isotherms were performed using various initial BPA solutions ranging from 5 to 200 mg L^{-1} at a fixed adsorbent dosage and were agitated for 1440 min, which is the optimum time. The thermodynamics experiments were also evaluated at temperatures of 293, 298, 303, 308 and 313 K. Kinetic and isotherm models were used to fit the experimental data using non-linear equations. All models and formulas are given in the results section.

After each study, 2 mL of the suspensions were extracted and filtered using syringe filters with a pore size (0.45 μm), transferred into a cuvette. Then, a double-beam UV–visible spectrophotometer (SPECORD 250 PLUS, Analytik Jena AG) measured the absorbance at the corresponding ($\lambda_{max} = 276$) wavelength. The linearity of Beer-Lambert law was checked for BPA concentration ranging from 5 to 200 mg L^{-1} with a correlation coefficient $R^2 = 0.9999$. The equilibrium adsorption capacity q_e (mg/g) and the removal rate R (%) were calculated as follows (Eqs. (1) and (2)):

$$q_e = (C_0 - C_e) * V / m \tag{1}$$

$$R\,(\%) = (C_0 - C_e) / C_0 * 100 \tag{2}$$

C_0 and C_e (mg/L) are the initial and equilibrium pollutant concentrations, respectively. V (L) is the volume of the solution, and m (g) is the adsorbent amount.

The regeneration performance of the saturated adsorbents was evaluated by washing with ethanol as a desorption eluent. The first adsorption was carried out using the optimised adsorption conditions. Afterwards, saturated PC-H and PC-Z were immersed in 50 ml ethanol solution and stirred for 2 h at 293 K. Next, the BPA-loaded adsorbent was filtered and washed thoroughly with osmosis water, dried in an oven, and used for the next adsorption cycle. The same adsorption-regeneration was further repeated for five consecutive cycles.

3. Results and discussion

3.1. Characterisation of activated carbons

3.1.1. Thermogravimetric (TG-DTA) analysis

Fig. 2 depicts the thermogravimetric (TG) and derivative thermogravimetric (DTA) curves of raw pine cone (PC) from room temperature to 973 K in the air. Fig. 2 shows the TG curve has three main weight losses when the temperature increases. The initial mass loss of 2.23 % (below 423 K) indicates the release of moisture, residual volatile content, and hydrocarbon [33,34]. The highest weight loss, of 48.92 %, was noticed between 473 and 613 K, and a steep weight loss of 42.17 %, was observed between 613 and 843 K, indicating thermal decompositions of various biomass components as volatile matter, including the hemicelluloses, cellulose, and lignin. The DTA profile exhibits two main weight-loss steps between 473 and 843 K. The first devolatilisation occurred between 473 and 613 K with a maximum weight loss rate of 593 K, and the second took place between 613 and 833 K with a maximum weight loss rate of 753 K, showing a sharp weight decrease. Thus, the first peak is related to hemicellulose and cellulose degradation, and the second mass loss to a relevant contribution from lignin and char degradation [35]. Above 843 K, no further mass reduction was noticed, revealing that the basic carbon structure was formed. The TG-DTA profiles described in the literature using pine cones as a precursor [33,35,36] are comparable to those found in the present work.

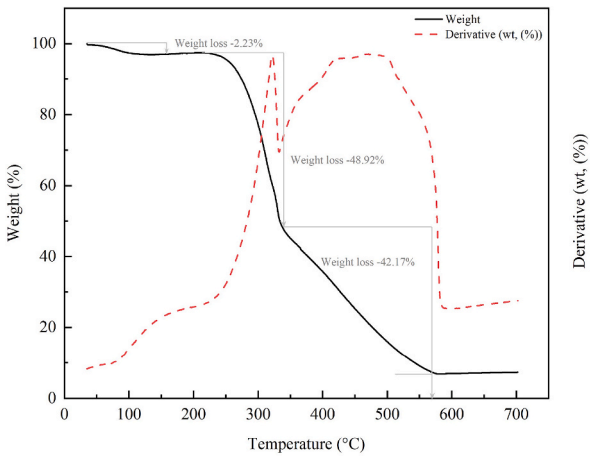

Fig. 2. TG and DTA curves of pine cone (in air, 10 °C min^{-1}).

3.1.2. FTIR analysis

The FTIR analysis was used to analyse and determine the surface functional groups of pine cones derived activated carbons along with the raw material in the range of 400–4000 cm^{-1}, and the results are depicted in Fig. 3.

The FTIR spectra for the pine cone sample (PC) present a wide range of peaks of varying intensity. The highest peak observed at 1025 cm^{-1} was assigned to C–O stretching in alcohol and asymmetric stretching of ester and ether functional group [17], whereas the band around 3300 cm^{-1} could be attributed to stretching vibrations of H bonded hydroxyl groups from phenols, carboxyls and alcohols or the presence of moisture content in the material [37]. Accordingly, this band is not visible in the spectra of the PC-H and PC-Z samples due to thermal carbonisation where the volatiles are released. The peak at 2930 cm^{-1} accounts for asymmetric and symmetric C–H stretching vibration for aliphatic groups [38], and the peak at 1612 cm^{-1} is related to the combination of the C═C stretching vibrations of the aromatic ring and the conjugated systems such as the diketone, the ketoester, the quinone [15]. The peak near 1370 cm^{-1} is related to COO- vibrations [37]. As expected, the spectra of activated carbons prepared after activation with H_3PO_4 and $ZnCl_2$ are simplified, with missing peaks due to the liberation of functional groups and volatiles during the carbonisation. Both activated carbons displayed similar surface chemical groups. Peaks at about 750–876 cm^{-1} can be associated with the C-H bending of aromatic structures, the peaks at 2355 cm^{-1} observed in the spectra of all samples correspond to the presence of the C≡;N bond, whereas for PC-H and PC-Z a moderate peak can be seen at 1550 cm^{-1} which can be related to oxygen functionalities, such as C–O stretching and conjugated C═O stretching in carboxylic groups [39].

3.1.3. XRD analysis

The crystal structure of prepared PC-H and PC-Z were analysed by X-ray diffraction (XRD); the adsorbents' diffraction patterns are presented in Fig. 4. The results showed that both samples display similar profiles, with two broad diffraction peaks centred at 2θ values of 24° and 42°, which are assigned to the (002) and (100) crystal planes of graphitic carbon, respectively, showed that the structure of the obtained ACs corresponded to typical amorphous carbon and graphite [40,41] which can be explained by the rupture of C-C bonds on the surface during preparation. Therefore, the prepared ACs can be considered as materials with disorganised structures [42], which help produce adsorbents with more developed pore structures, making them ideal for the adsorption of various contaminants. These results are in line with the research studies by Sharafinia et al. [41], Zhang et al. [43], and Shi et al. [22].

3.1.4. SEM analysis

To investigate the change in surface morphology after activation, scanning electron microscopy (SEM) characterisation was performed on PC-H (Fig. 5A–B) and PC-Z (Fig. 5C–D) at × 2500 and × 3500 magnifications. The SEM images of activated samples PC-Z and PC-H exhibit a significant distinction in the microscopic morphology and porous structure with different sizes and shapes [44]. Both materials show a hierarchical porous structure with several pore sizes and rough surfaces. Although, PC-Z sample featured an irregular surface with different pore volumes, distributed randomly (Fig. 5C–D), while PC-H had an extremely uniform size distribution with a large number of pores (Fig. 5A–B), these characteristics were consistent with the higher specific surface area and average pore diameter as indicated by the BET analysis. Overall, H_3PO_4 and $ZnCl_2$ activation seems to have a significant impact on enhancing the morphology of pine cones carbon.

3.1.5. BET analysis

The materials' specific surface area (SSA) and pore characteristics before and after chemical activation have been evaluated. The N_2 adsorption-desorption isotherm curves for activated samples are presented in Fig. 6-A, whereas the pore size distribution by the BJH method is illustrated in Fig. 6-B. Calculated SSAs, pore volume and pore size for PC, PC-H and PC-Z are listed in Table 2. Results showed

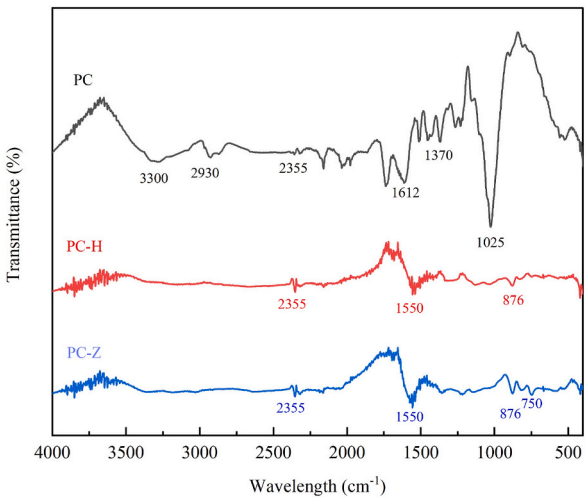

Fig. 3. FTIR spectra of PC, PC-H and PC-Z.

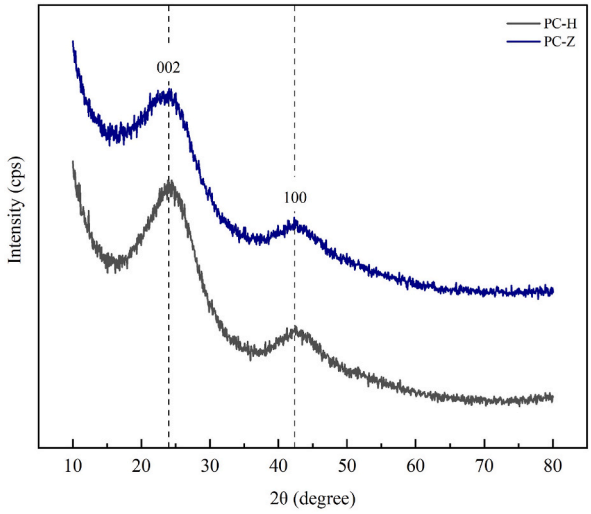

Fig. 4. XRD patterns of activated carbons.

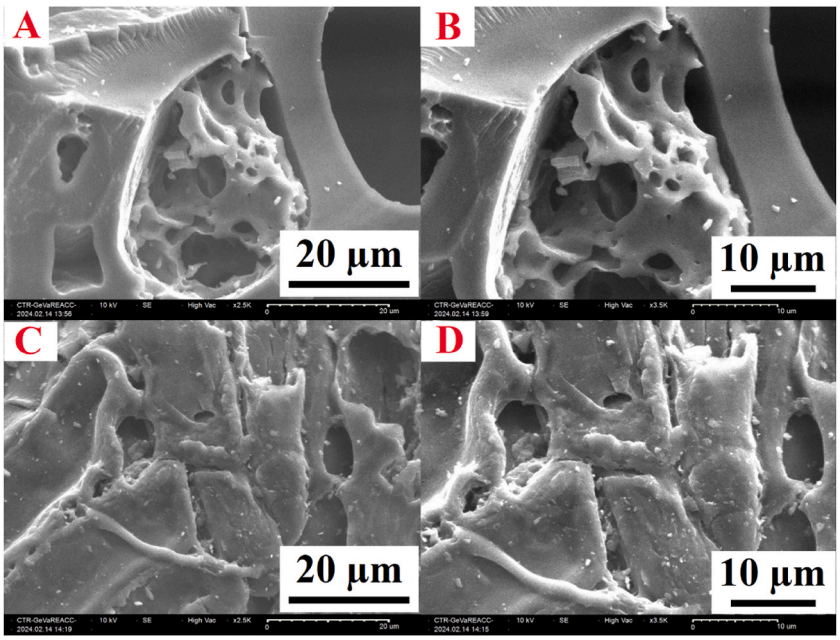

Fig. 5. SEM micrographs with different magnifications of PC-H (A–B) and PC-Z (C–D).

that both PC-H and PC-Z present higher SSAs (1369.03 m^2/g and 1018.86 m^2/g, respectively), pore volume (0.12 cm^3/g and 0.37 cm^3/g, respectively) and the average diameter (2.65 nm and 3.01 nm, respectively) compared to the raw material (Table 2). Nitrogen adsorption-desorption isotherms indicated that the materials show intermediate characteristics between type 1 and 4 isotherms, according to the International Union of Pure and Applied Chemistry (IUPAC) classification [45], which confirms the contribution of a mixture of micropores and mesopores in the porous structure of the studied ACs. BJH average pore diameter of PC-Z was higher than PC-H which may be due to the formation of macro- and mesopores in the PC-Z surface.

On the other hand, Fig. 6-B illustrates the pore size distributions of ACs by the BJH method. Both samples had different pore size distributions, with most of the pores concentrated between 2 nm and 5 nm. Compared with PC-Z, the number of micropores/small mesopores in the PC-H structure was significantly higher. Moreover, the dimensions of emerging organic molecules are accessible to the carbon micropores. This suggests that micropores/small mesopores and the extent of their volume are important for the adsorption of these kinds of substances. Indeed, the trend of their adsorbed amount depends on the predominance of smaller pores in the sample, which can enhance the adsorption capacity [45,46]. The BET and BJH analysis results show that the prepared ACs have different SSAs and pore volumes, which are expected to have various adsorption capacities for bisphenol A.

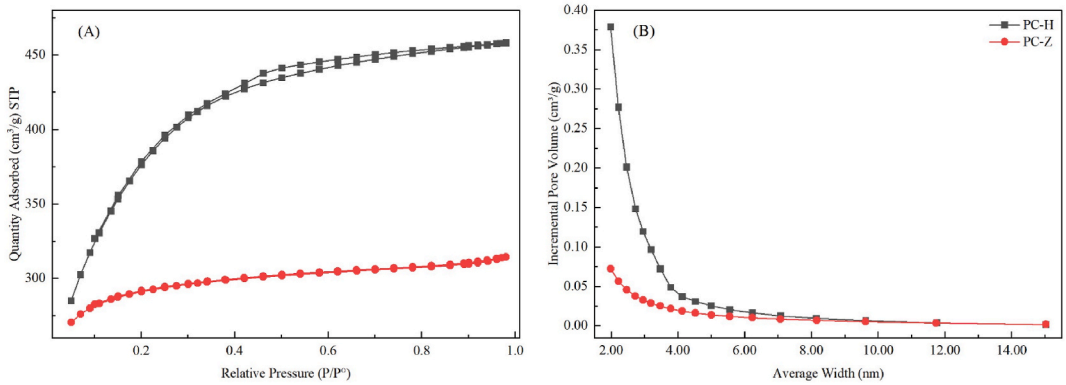

Fig. 6. (A) Nitrogen adsorption-desorption isotherms at 77 K for samples activated carbon, and (B) Incremental pore volumes by BJH desorption branch of the isotherm.

Table 2
Surface area (S_{BET}) and pore characteristics of PC, PC-H and PC-Z.

Adsorbents	BET Surface Area (m^2/g)	t-Plot micropore volume (cm^3/g)	BJH Desorption average pore width (nm)
PC	0.15	0	11.50
PC-H	1369.03	0.12	2.65
PC-Z	1018.86	0.37	3.01

3.2. Adsorption experiments of BPA

3.2.1. Effect of adsorbent dose

Fig. 7 shows the effect of the adsorbents dose on BPA adsorption. The removal efficiency increased with the increase of the adsorbent dose till the dose of 0.04 g and 0.1 g for PC-H and PC-Z, respectively, with up to 96 % of removal efficiency. This can be attributed to the increase in adsorbents surface area and the presence of more adsorption sites [17]. However, further increases in the adsorbent dosage had no significant changes in the removal efficiency. A similar finding was also reported for phenol adsorption by biochar prepared from pine fruit shells [38]. These results can also be explained by the high specific surface area of PC-H compared to PC-Z which leads to saturation of the material with a lower adsorbent mass. Therefore, the optimum adsorbent dosage was 0.04 g for PC-H and 0.1 g for PC-Z for subsequent adsorption experiments.

3.2.2. Effect of pH

During the adsorption study, pH variation is a key factor as it can alter the surface properties of the adsorbent and the pollutant molecules, and thus influence the adsorption process [47]. BPA is a weak acid with a pKa value of 10.3 [48]. The effect of the initial pH

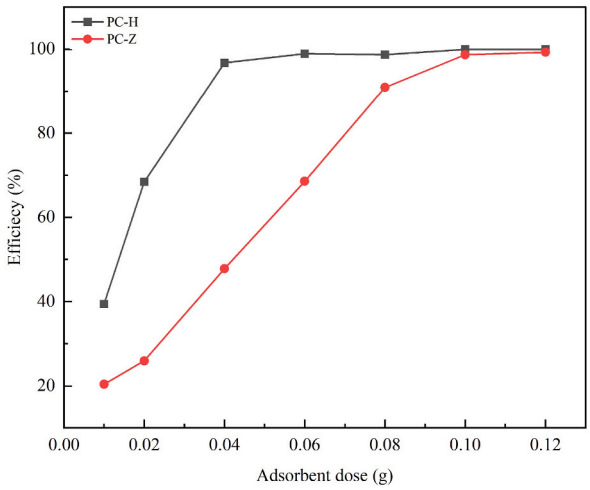

Fig. 7. Effect of adsorbent dose on BPA adsorption (solution volume = 100 ml, initial concentration = 50 mg L^{-1}, temperature = 293 K, pH = 6.7).

of the BPA solution on adsorption by PC-H and PC-Z in the range of 2–12 was investigated (Fig. 8A). The results showed that both activated carbon adsorption capacity toward BPA remained quite stable at pH between 2 and 10. For a pH value exceeding 10, the adsorbed amount dropped rapidly. The amount of BPA adsorbed gradually decreased between pH 10 and 12 by 50.4 % for PC-H (from 121 to 61 mg/g) and by 26 % for PC-Z (from 50 to 37 mg/g).

Regarding the literature, it was reported that when pH was below the dissociation constant of the pollutant (pKa (BPA) = 10.3), most of the BPA molecules in the solution were neutral and could be adsorbed by hydrogen bonding [22]. As the pH of the solution increases, neutral BPA is gradually deprotonated to BPA^{-} and BPA^{2-}. Thus, the hydrophobic interactions of BPA^{-} and BPA^{2-} with PC-H and PC-Z decreased with increasing pH, which may inhibit the adsorption of BPA at higher pH solutions [49]. Therefore, the adsorption of BPA by the prepared activated carbons is maximum in the pH range of 2–10, as hydrogen bonding was dominant between the adsorbents and the molecule. Therefore, adsorption isotherms, kinetics, thermodynamic parameters, and regeneration experiments are determined using an initial pH solution (between 6 and 7).

The surface nature of prepared adsorbents was determined by the parameter pH point of zero charges (pHpzc) method. The pHpzc of the PC-H and PC-Z are 5.8 and 6.8, respectively as presented in Fig. 8B. Results show that all the pHpzc of the synthesised ACs is less than 7, signifying the domination of acid groups on the adsorbents' surface. Therefore, chemical activation leads to the formation of oxygenated groups of an acidic nature on the surface of the activated carbons. The high BPA removal between pH 2.0 and 6.8 indicates the active role played by the positively charged groups on carbons, Above pH 6.8, functional groups on the surface of the adsorbents would impart an overall negative charge due to OH^{-} functional groups that could be involved in electrostatic interactions with BPA. However, a marked reduction in BPA uptake was recorded above pH 10.0. As discussed earlier, the molecular form of BPA could interact with the charged surface of the carbonaceous materials at high pH. Given that the adsorbents (PC-H and PC-Z) and adsorbate (BPA) are negatively charged above pH 10. The found pHpzc is comparable to others found in the literature. For instance, the pHpzc of microalga Chlorella sp. derived AC activated with K_2CO_3 was 5.21 [50].

3.2.3. *Effect of initial concentration - adsorption isotherms*

The effect of initial BPA content on BPA adsorption on prepared adsorbents in the range of 5–200 mg L^{-1} was studied at a fixed adsorbent dosage of 0.4 g L^{-1} and 1 g L^{-1} for PC-H and PC-Z, respectively, and pH 6.7. Fig. 9-A displays the amount of adsorbed BPA (Q_e) as a function of the aqueous medium's equilibrium concentrations (C_e). As shown in Fig. 9-B, the absorption capacity of BPA increased from 13.07 to 216.92 mg g^{-1} and 5.19–73.53 mg g^{-1} for PC-H and PC-Z, respectively, upon increasing the BPA concentration within the range of 5–200 mg L^{-1}. Therefore, increasing the BPA initial concentration produced a higher driving force between the adsorbent surface and the molecule, promoting rapid mass transfer [51]. At all concentrations, the adsorption capacity of PC-H on BPA was significantly higher than that of PC-Z due to its unique structure and higher surface area.

Equilibrium isotherms were obtained to evaluate the adsorption capacity of BPA for each prepared carbon. Adsorption isotherm studies are essential and provide in-depth knowledge of how the adsorbed molecules distribute between liquid solutions and the surface of the adsorbent at equilibrium. Therefore, they used to understand the adsorption mechanism and select the appropriate adsorbent [52]. The most prevalent adsorption isotherm models, Langmuir (Eq. (3)), Freundlich (Eq. (4)), and Temkin (Eq. (5)), were applied to analyse equilibrium data for the adsorption of bisphenol A on activated carbons. The linear representation of the isotherm models is expressed below:

Langmuir isotherm model:

$$C_e / q_e = K_L/q_{max} + C_e/q_{max} \tag{3}$$

Freundlich isotherm model [53]:

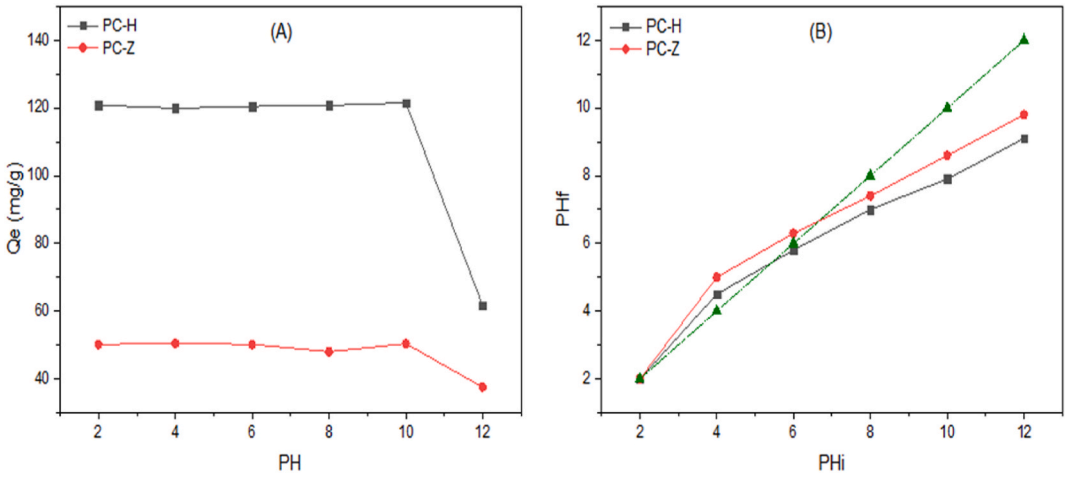

Fig. 8. (A) Effect of pH on the amount of BPA adsorbed (solution volume = 100 ml, temperature = 293 K, adsorbent dose = 0.04 g (for PC-H) and 0.1 g (for PC-Z), initial concentration = 50 mg L^{-1}), (B) pH point of zero charge of PC-H and PC-Z.

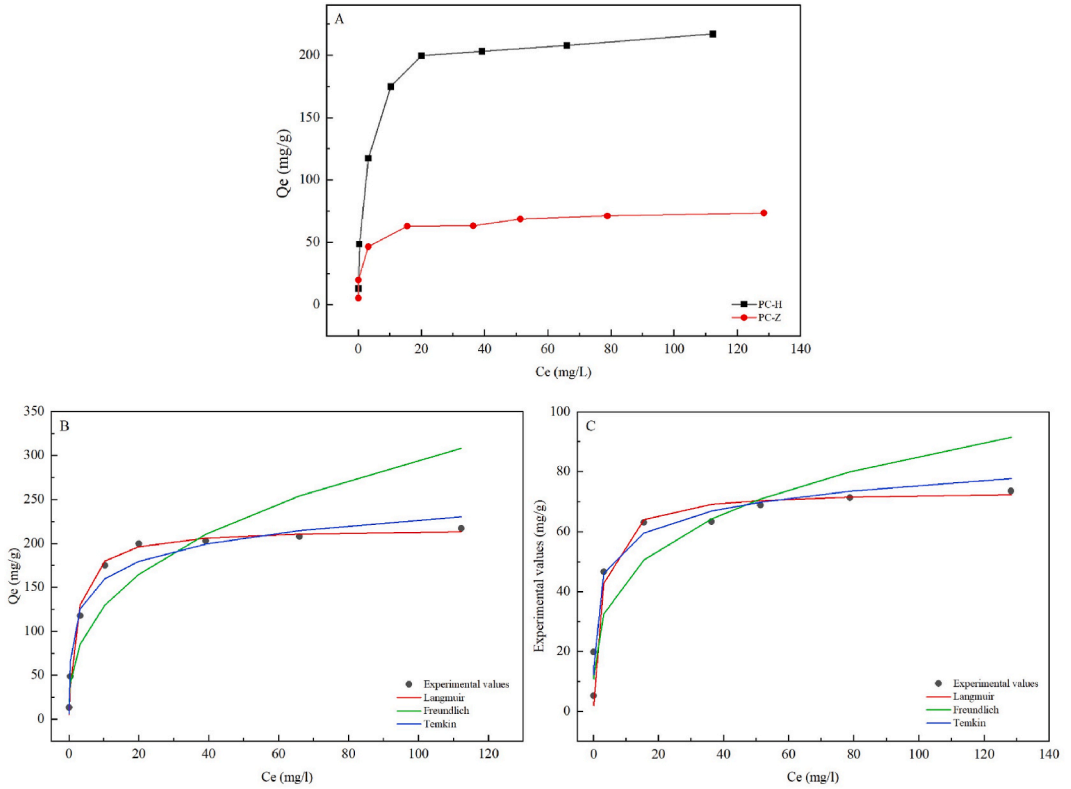

Fig. 9. (A) Effect of initial concentration on adsorption of BPA, and adsorption isotherms of BPA on (B) PC-H and (C) PC-Z.

$$log\ q_e = log\ C_e/n_F + log\ k_F \tag{4}$$

Temkin isotherm model [54]:

$$q_e = ln\ A_T * RT/b_T + ln\ C_e * RT/b_T \tag{5}$$

where q_e is the uptake of BPA per unit weight of the carbon (mg/g), q_{max} is the maximum BPA uptake (mg/g), C_e is the residual concentration of BPA at the equilibrium (mg L^{-1}), K_L is the Langmuir constant (L/mg), K_F is the Freundlich constant (mg g^{-1} (L mg^{-1}) 1/n), $1/n_F$ is the intensity of the adsorption, A_T (L g^{-1}) is the Temkin isotherm constant and b_T (J mol^{-1}) is associated to the heat of adsorption.

Fig. 9B-C shows the adsorption isotherms of BPA by PC-H and PC-Z, as well as data fit by using Langmuir, Freundlich, and Temkin models, also the parameters of these three isotherms, along with the corresponding R^2 are shown in Table 3. As commented, the values of R^2 of the Langmuir isotherm in all cases were higher than that of the Freundlich and Temkin isotherms. Furthermore, the value $1/n_F$ less than one suggests that the adsorption process is normal Langmuir. These results further demonstrate that the Langmuir model better represents the adsorption equilibrium of BPA on the two activated carbons, suggesting that the adsorption occurs on the surface of the materials as homogeneous monolayer adsorption [24,39]. The maximum monolayer adsorption capacity (q_{max}) at 293 K was 217.39 mg g^{-1} and 73.53 mg g^{-1} for PC-H and PC-Z, respectively. Meanwhile, PC-H has shown a much higher adsorption capacity than PC-Z prepared under similar conditions.

Table 3
Isotherm parameters calculated for BPA adsorption.

Materials	Langmuir	Freundlich	Temkin
PC-H	q_{max} = 217.39	k_F = 55.768	b_T = 82.739
	k_L = 0.4646	n_F = 2.7616	A_T = 22.19
	R^2 = 0.9994	R^2 = 0.9157	R^2 = 0.9717
PC-Z	q_{max} = 73.53	k_F = 23.432	b_T = 284.147
	k_L = 0.4359	n_F = 3.5612	A_T = 67.1279
	R^2 = 0.9982	R^2 = 0.8281	R^2 = 0.976

3.2.4. Effect of contact time - kinetics study

The contact time for the adsorption of the Bisphenol A molecules on the prepared adsorbents plays a crucial role in the adsorption process, as it explains the time taken to reach equilibrium as well as the diffusion of the adsorbate into the pores of the adsorbent. The adsorption data for the uptake of BPA as a function of contact time onto PC-H and PC-Z at a constant initial concentration is illustrated in Fig. 10-A. A two-stage kinetic behaviour accompanies the adsorption of BPA on two activated carbons: initially, the adsorbed amount increases significantly up to 24 h, followed by a second stage with a quasi-stable removal rate for 24–30 h. In fact, the steep increase in adsorption efficiency during the initial adsorption phase induces a large number of adsorption sites available and, thus an increase in the mass transfer rate from the solution to the adsorbent surface [55]. However, a second stable phase is observed. During this phase, a saturation level is obtained due to the occupation of the adsorbent sites by the BPA molecules. This reveals that equilibrium is established after 24 h for BPA solutions at 50 mg. L^{-1}.

To better understand the adsorption mechanism, mathematical models corresponding to the present adsorption study were used to simulate the adsorption kinetics of BPA by applying the pseudo-first-order (Eq. (6)) and the pseudo-second-order kinetic models (Eq. (7)):

Pseudo-first-order model:

$$log(q_e - q_t) = log\ q_e - k_1 t \tag{6}$$

Pseudo-second-order model:

$$t\,/\,q_t = 1/K_2 q_e^2 + t/q_e \tag{7}$$

where q_e (mg/g) and q_t (mg/g) are the adsorption amounts of bisphenol A at equilibrium and time t, k_1 (min^{-1}) and k_2 (g mg^{-1} min^{-1}) are the equilibrium rate constants of the pseudo-first-order and pseudo-second-order models.

The kinetic models, pseudo-first order and pseudo-second order were used to fit the experimental data and plots are shown in Fig. 10-B and C. Table 4 lists the kinetic parameters derived from the fits of the two models and the corresponding coefficients of determination, R^2. The results reveal that the pseudo-second-order model describes the adsorption process for BPA by PC-H and PC-Z well, as the R^2 value was found to be highest compared to the R^2 of the pseudo-first-order model. Furthermore, the adsorbent amount at equilibrium ($q_{e,\ exp}$) was found to be closer to the experimental value in the case of pseudo-second-order kinetics [56,57]. Thus, BPA adsorption by our adsorbents fits the pseudo-second-order kinetics better, which indicates that the adsorption process is mainly a monolayer process dominated by physisorption [58]. Besides, the hierarchical structure and the significant S_{BET} results showed that the adsorption capacities of PC-H (126.58 mg g^{-1}) are much higher than those of PC-Z (58.48 mg g^{-1}), indicating a faster PC-Z

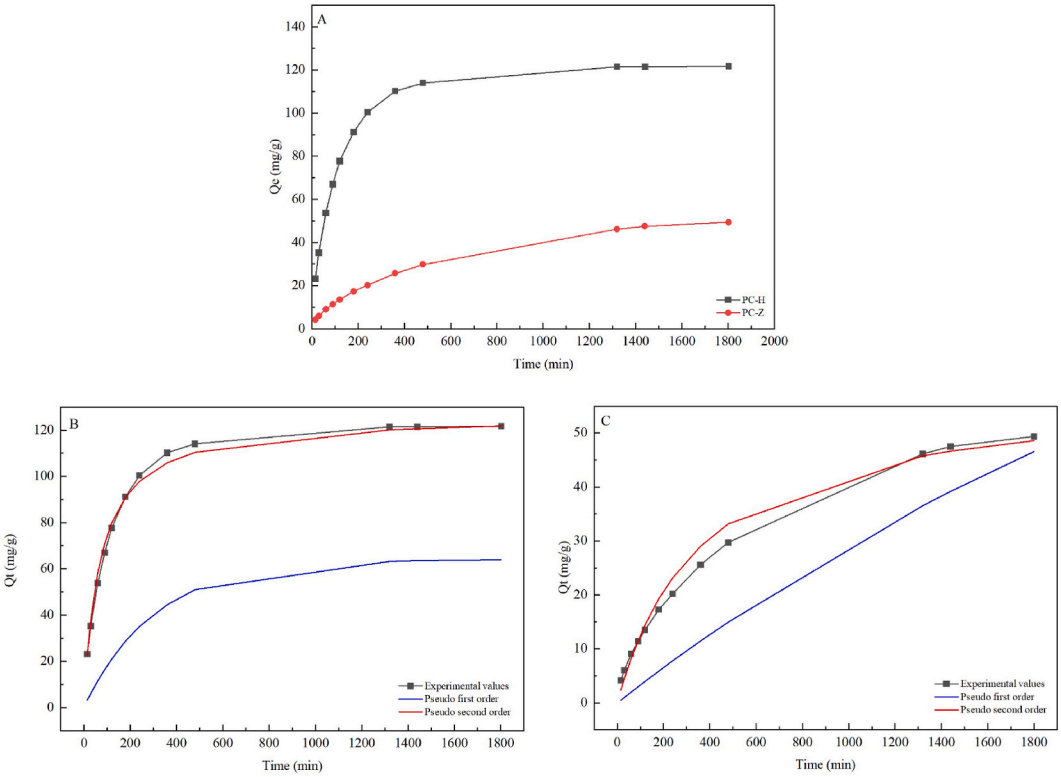

Fig. 10. The adsorption performance of BPA (A), pseudo-first-order and pseudo-second-order kinetics model of BPA onto PC-H (B) and PC-Z (C).

Table 4
Fit parameters of Pseudo-first order and Pseudo second order kinetics for experimental BPA data.

Materials	$q_{e,\ exp}$ (mg g^{-1})	Pseudo first order	Pseudo second order
PC-H	121.9	$q_e = 64.08$	$q_e = 126.58$
		$k_1 = 0.0033$	$k_2 = 0.0140$
		$R^2 = 0.9649$	$R^2 = 0.9998$
PC-Z	50	$q_e = 111.63$	$q_e = 58.48$
		$k_1 = 0.0003$	$k_2 = 0.0027$
		$R^2 = 0.9485$	$R^2 = 0.9829$

saturation.

3.2.5. Thermodynamic study

To investigate the internal energy changes during the adsorption process of BPA. Thermodynamics parameters, including Gibbs free energy change (ΔG^o), standard enthalpy variation (ΔH^o) and entropy change (ΔS^o) were calculated based on the effect of temperature within the range 293–313 K. It can provide valuable information on the mechanism of the underlying processes and the energetic changes. The values of ΔS° and ΔH° for BPA adsorption were determined from the intercept and slope of the plot between $\ln K_d$ versus 1/T. The thermodynamic variables (ΔG^o, ΔH^o, and ΔS^o) were calculated using the following formulas (Eqs. (8)–(11)):

$$K_d = q_e / C_e \tag{8}$$

$$\Delta G^\circ = -RT \ln K_d \tag{9}$$

$$\Delta G^\circ = \Delta H^\circ - T\Delta S^\circ \tag{10}$$

$$\ln K_d = \Delta S^\circ / T - \Delta H^\circ / RT \tag{11}$$

where K_d is the thermodynamic distribution coefficient, q_e (mg·g^{-1}) is the amount of BPA adsorbed at equilibrium and C_e (mg·L^{-1}) is the concentration of BPA at equilibrium, R represents the universal gas constant (8.314 J mol^{-1} $^\circ K^{-1}$), and T (°K) is the system temperature.

Table 5 shows the calculated thermodynamic parameters of the adsorption of BPA on prepared adsorbents at temperatures of 293, 298, 303, 308 and 313 K. Both PC-H and PC-Z showed negative standard free energies (ΔG^o) at all temperatures, indicating that the biosorption of BPA onto activated carbons was thermodynamically spontaneous. As shown in Table 5, the ΔG^o values became more negative as the temperature increased from 293 to 313 K, indicating a greater affinity of the adsorbents toward BPA at higher temperatures. In addition, the (ΔG^o) value of the tested samples was less than 40 kJ mol^{-1}, confirming that the adsorption process was governed by a physical adsorption mechanism [38]. Furthermore, the positive values of standard enthalpy variation (ΔH^o) reflect an endothermic nature of the adsorption process, and the positive entropy change (ΔS^o) values indicated an increase in the randomness at the solution-adsorbent interface throughout BPA adsorption development. Moreover, the (ΔS^o) value for PC-H (0.135 kJ $mol^{-1}K^{-1}$) was relatively low compared to that of PC-Z (0.251 kJ $mol^{-1}K^{-1}$), suggesting an increase in affinity between BPA molecules and PC-H [39,59].

3.3. Desorption-regeneration studies

In any adsorption process, the regeneration step is essential to determine the adsorbent's durability and economic viability. Thus, different desorption agents have been studied for BPA desorption, including HCl, NaCl, NaOH, Ethanol, and Methanol [28,39], among which ethanol showed high desorption efficiency for BPA bound by hydrophobic interaction, making it a better desorption solvent. Therefore, the regeneration of the exhausted PC-H and PC-Z loaded with BPA was conducted for up to five cycles using desorption solutions of ethanol. Initially, 0.04 g and 0.1 g of PC-H and PC-Z were stirred with 100 ml of 50 mg L^{-1} BPA solution until equilibrium

Table 5
Thermodynamic parameters of BPA adsorption onto PC-H and PC-Z at different temperatures.

Adsorbent	T (°K)	Ln K_d	ΔG° (KJ mol^{-1})	ΔH° (KJ mol^{-1})	ΔS° (KJ mol^{-1} K^{-1})
PC-H	293	3.474	−8.445	31.125	0.135
	298	3.651	−9.121		
	303	3.876	−9.796		
	308	4.169	−10.471		
	313	4.235	−11.146		
PC-Z	293	2.234	−4.876	68.837	0.251
	298	2.327	−6.134		
	303	2.507	−7.392		
	308	3.727	−8.650		
	313	3.800	−9.908		

for saturation of the adsorbents. Then, saturated carbons were immersed in 50 ml of ethanol solution and stirred for 2 h at 298 K. They were then filtered and washed several times with osmosis water, oven-dried at 353 K, and used again for the next BPA adsorption. The results of five consecutive adsorption–desorption experiments are graphically presented in Fig. 11. It can be observed that the amount of adsorbed BPA decreased slightly after five-time regeneration. Hence, the initial BPA removal rate was reduced by 4.47 % and 9.42 % for PC-H and PC-Z, respectively, after 5 successive cycles, remaining at about 80.33 % and 57.68 % of the first adsorption capacity. This slight decrease in adsorption capacity could be attributed to the occupation of the binding sites by BPA molecules, which can block some pores. The results confirm that the current adsorbents can be reused at least five times, which could eventually prove to be economically viable.

3.4. Possible adsorption mechanism of BPA

The adsorption of BPA by carbon adsorbents is generally determined by the adsorbent's textural (microstructure) and surface properties. PC-H and PC-Z exhibited a very high SSA and microporosity, which is confirmed by the BET and SEM analysis. This promotes the diffusion and adsorption of BPA. Thus, the possible mechanisms of BPA uptake by ACs may be assumed as follows:

- First, the solute molecules are transported from the bulk solution to the boundary layer, with subsequent diffusion from the boundary layer to the external surface of the adsorbent (external diffusion), and then to the surface pores (intraparticle diffusion).
- Second, the uptake of BPA molecules occurs in the pores of the carbonaceous materials.

The desorption/regeneration process results indicated that physical interactions were very likely between BPA and the adsorbents, as only a small number of BPA molecules remained on the AC's surface.

The hydrogen bonds are an important factor that may play a key role in the uptake of BPA. As reported by de Lima et al. [39], the hydroxyl groups of BPA and the oxygen groups of the Acs may have formed hydrogen bonds. FTIR spectra of activated samples indicated a moderate peak at 1550 cm^{-1} which can be related to oxygen functionalities, such as C-O stretching and conjugated C═O stretching in carboxylic groups. This outcome shows that hydrogen bonds can be involved in BPA adsorption by PC-H and PC-Z, but they might not be the most significant force.

Further, the zero potential point was measured for both adsorbents and found to be close to the value of 6.8, with the surface of the ACs being positively charged at pH below 6.8. Electrostatic interactions between the ACs and BPA could occur at pH < 10, where the molecular form of BPA could interact with the charged surface of the adsorbents. The intermolecular force, such as π-π interaction between rings of the carbonaceous materials and electrons in BPA could also be a dominant mechanism for the adsorption of BPA. Some studies have confirmed that hydrophobic interaction represents an important mechanism in the adsorption of BPA. For example, it has been reported by Ndagijimana et al. [60] that the high value of the octanol-water partition coefficient ($logK_{ow}$) indicates a higher hydrophobic property which consequently increases the adsorption efficiency of bisphenols. In short, the possible mechanisms of BPA adsorption onto PC-H and PC-Z in batch mode may involve pore texture, hydrogen bonds, π-π interactions, electrostatic forces and hydrophobic interactions.

3.5. Comparison of prepared activated carbons with other existing adsorbents

The efficiency of the prepared materials was compared with other adsorbents reported in the literature. The BET surface area, maximum adsorption capacity, and operating conditions of BPA adsorption on different adsorbents (as parameters of comparison) are summarised in Table 6. PC-H material exhibits a better removal capacity, which outperforms some adsorbents. This shows that pine cones activated H_3PO_4, one of the good adsorbents and could be used as an alternative to activated carbon for BPA removal. The focus on green carbon-based local waste makes our study both environmentally friendly and effective for the Removal of emerging contaminants, especially BPA from water.

4. Cost analysis of the adsorbent

The production cost has been done by comparing the synthesised adsorbents (PC-H and PC-Z) with the cost of other commercially available carbons. In the present work, around 2.5 Kg of pine cones have been utilised to produce about 1 Kg of activated carbon (with a yield of 40 %). This estimation only includes the mass and energy consumption associated with (i) the raw material, (ii) the raw material preparation (washing and drying), and (iii) the adsorbent production (carbonisation, activation, neutralisation). However, the pine cones used in this study were collected locally without any associated cost.

The cost involved in the process was estimated based on the study carried out by Jaria and al [68]. on the economic costs of waste-based AC for application in water treatment and was found to be around 75.04€ for PC-H and 68.64€ for PC-Z. Sample collection 0€ (waste biomass), chemical activation (H_3PO_4 (50 %) = 45.6€; $ZnCl_2$ = 39.2€), carbonisation at Nitrogen atmosphere heating (773 K, 90 min, flow rate 100 ml/min = 10.24€), washing and drying (13.2€), grinding and neutralisation (4.8€), electricity (1.2€). Table 7 shows the comparative study of the prepared adsorbents with commercial carbons.

According to the above, it can be seen that the cost of the prepared activated carbon is quite lower as compared to the commercially available carbons, suggesting that pine cone biomass can serve as a cheaper precursor for the preparation of activated carbon. Demonstrate the possibility of producing cost-effective and environmentally friendly materials.

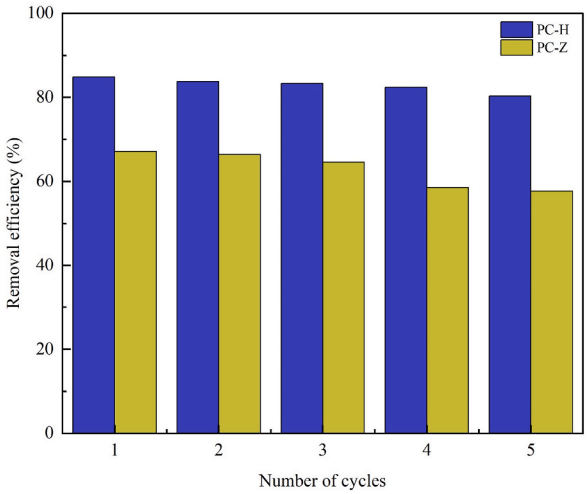

Fig. 11. Recyclability of PC-H and PC-Z.

Table 6
Comparison of the adsorption capacity of BPA on pine cone-based activated carbons with other agro-waste adsorbents.

Adsorbent	BET surface area (m^2/g)	Maximum adsorption q_m ($mg\ g^{-1}$)	Conditions			Reference
			Adsorbent dosage ($g\ L^{-1}$)	PH	T (°K)	
Activated carbon from kraft lignin	1053	220	0.36	–	298	[56]
Oil palm empty fruit bunch	86.62	41.98	1.5	2–9	–	[61]
Coconut shell-based hydrophobic MAC modified with nanoscale zero-valent iron (NZVI@MAC)	933.12	327.60	0.2	3–9	298.15	[62]
Corn cob	–	51.25	0.2	3–7	–	[63]
Activated carbon from Tithonia diversifolia	854.44	15.69	0.2	7	298	[64]
Palm shell	770	45.45	–	3	303	[65]
Coffee grounds	1039	123.2	–	2–4	–	[66]
Rice straw activated carbon treated with KOH	1304.8	181.19	0.1	2.35	303	[67]
Pine cones activated $ZnCl_2$	1018.86	73.53	1	2–10	298	**Present study**
Pine cones activated H_3PO_4	1369.03	217.39	0.4	2–10	298	**Present study**

Table 7
Cost Analysis of PC-H and PC-Z with some other commercial activated charcoal.

	PC-H	PC-Z	Activated Charcoal Norit	Norit*SX2	DARCO*
Surface area (m^2/g)	1369.03	1018.86	~900-1000	~900-1000	~600
Cost/1 Kg (in €)	75.04	68.64	241	133.4	141

5. Conclusion

In this study, porous activated carbons from Moroccan pine cones were successfully uptake, synthesised, and used as adsorbents to uptake an emerging contaminant (BPA) from water. The experimental adsorption results of the present research can be summarised as follows:

1) Porous activated carbons with a high BET surface area (1369.03 $m^2\ g^{-1}$ and 1018.86 $m^2\ g^{-1}$) were prepared via chemical activation of PC followed by carbonisation, using H_3PO_4 and $ZnCl_2$ as the activating agent.
2) The lab-scale adsorption studies revealed that the maximum adsorption performances (> 96 %) of BPA were obtained at neutral pH, initial BPA concentration of 50 mg L^{-1}, a retention time of 24 h, and PC-H and PC-Z dosage of 0.4 g L^{-1} and 1 g L^{-1}, respectively.

3) Equilibrium adsorption experiments revealed that PC-H showed the highest BPA uptake values (217.39 mg g^{-1}), compare to PC-Z adsorption capacity (73.53 mg g^{-1}), which could be attributed to PC-H large specific surface area and micropore volume which facilitate the capture of BPA.
4) The adsorption of BPA by both samples followed the pseudo-second-order model, whereas BPA isotherms were satisfactorily fitted to the Langmuir model, suggesting that the adsorption of BPA is homogeneous monolayer adsorption. Furthermore, the thermodynamic parameters confirmed that the adsorption process was spontaneous and endothermic.
5) Used PC-H and PC-Z could be easily regenerated up to five cycles using ethanol as a desorption agent.
6) The possible mechanisms by which prepared materials adsorbed BPA may involve the pore texture, hydrogen bonds, hydrophobic interaction, electrostatic forces, π-π interaction.

Therefore, the present study proves that porous activated carbon prepared from pine cones would make a promising low-cost adsorbent because of its high surface area and adsorption behaviour towards emerging contaminants in the prospect of future application in large-scale wastewater treatment technologies.

CRediT authorship contribution statement

Yassine Jari: Writing – review & editing, Writing – original draft, Methodology, Investigation, Conceptualization. **Nicolas Roche:** Writing – review & editing, Writing – original draft, Supervision, Investigation, Funding acquisition. **Mohamed Chaker Necibi:** Writing – review & editing, Writing – original draft, Supervision, Methodology, Investigation, Funding acquisition. **Fatima Zahra Falil:** Investigation. **Saida Tayibi:** Writing – original draft. **Karim Lyamlouli:** Investigation. **Abdelghani Chehbouni:** Project administration, Funding acquisition. **Bouchaib Gourich:** Writing – review & editing, Writing – original draft, Methodology, Investigation.

Declaration of competing interest

The authors declare that they have no known competing financial interests or personal relationships that could have appeared to influence the work reported in this paper.

Acknowledgements

The authors are grateful to the Mohammed VI Polytechnic University (UM6P) of Benguerir and the OCP Foundation for supporting this research work and would like to thank the Laboratory of Process and Environmental Engineering, Higher School of Technology, Hassan II University, Morocco for putting at our disposal the necessary equipment for this study. Particular thanks to YAMARI Imane for the characterisation.

References

[1] Journal of Environmental Chemical Engineering S. Khan, M. Naushad, A. Al-gheethi, J. Iqbal, Engineered nanoparticles for removal of pollutants from wastewater : current status and future prospects of nanotechnology for remediation strategies, J. Environ. Chem. Eng. 9 (2021) 106160, https://doi.org/10.1016/j.jece.2021.106160.
[2] E. Menya, J. Jjagwe, H. Mpagi, Progress in deployment of biomass-based activated carbon in point-of-use filters for removal of emerging contaminants from water : a review, Chem. Eng. Res. Des. 192 (2023) 412–440, https://doi.org/10.1016/j.cherd.2023.02.045.
[3] S.A. Mirzaee, Z. Noorimotlagh, M. Ahmadi, F. Rahim, S.S. Martinez, A. Nourmohammadi, N. Jaafarzadeh, The possible oxidative stress and DNA damage induced in Diclofenac-exposed Non-target organisms in the aquatic environment: a systematic review, Ecol. Indicat. 131 (2021) 108172, https://doi.org/10.1016/j.ecolind.2021.108172.
[4] Journal of Environmental Chemical Engineering P. Bhatt, G. Bhandari, M. Bilal, Occurrence , toxicity impacts and mitigation of emerging micropollutants in the aquatic environments : recent tendencies and perspectives, J. Environ. Chem. Eng. 10 (2022) 107598, https://doi.org/10.1016/j.jece.2022.107598.
[5] V.K. Parida, D. Saidulu, A. Majumder, A. Srivastava, B. Gupta, A.K. Gupta, Emerging contaminants in wastewater: a critical review on occurrence, existing legislations, risk assessment, and sustainable treatment alternatives, J. Environ. Chem. Eng. 9 (2021) 105966, https://doi.org/10.1016/j.jece.2021.105966.
[6] Y. Jari, N. Roche, M.C. Necibi, S. El Hajjaji, D. Dhiba, A. Chehbouni, Emerging pollutants in Moroccan wastewater: occurrence, impact, and removal technologies, J. Chem. (2022) 2022, https://doi.org/10.1155/2022/9727857.
[7] W.T. Vieira, M.B. De Farias, M.P. Spaolonzi, M.G.C. Da Silva, M.G.A. Vieira, Endocrine-disrupting compounds: occurrence, detection methods, effects and promising treatment pathways - a critical review, J. Environ. Chem. Eng. 9 (2021), https://doi.org/10.1016/j.jece.2020.104558.
[8] Journal of Environmental Chemical Engineering N. Boraah, S. Chakma, P. Kaushal, Attributes of wood biochar as an efficient adsorbent for remediating heavy metals and emerging contaminants from water : a critical review and bibliometric analysis, J. Environ. Chem. Eng. 10 (2022) 107825, https://doi.org/10.1016/j.jece.2022.107825.
[9] Science of the Total Environment M.V. López-ramón, R. Ocampo-pérez, M.I. Bautista-toledo, J. Rivera-utrilla, C. Moreno-castilla, M. Sánchez-polo, Removal of bisphenols A and S by adsorption on activated carbon clothes enhanced by the presence of bacteria, Sci. Total Environ. 669 (2019) 767–776, https://doi.org/10.1016/j.scitotenv.2019.03.125.
[10] Bioresource Technology P. Thaveemas, L. Chuenchom, S. Kaowphong, S. Techasakul, Magnetic carbon nanofiber composite adsorbent through green in-situ conversion of bacterial cellulose for highly efficient removal of bisphenol A, Bioresour. Technol. 333 (2021) 125184, https://doi.org/10.1016/j.biortech.2021.125184.
[11] Chemosphere F.M. Mpatani, A.A. Aryee, A.N. Kani, Q. Guo, E. Dovi, L. Qu, Z. Li, R. Han, Uptake of micropollutant-bisphenol A , methylene blue and neutral red onto a novel bagasse- b -cyclodextrin polymer by adsorption process, Chemosphere 259 (2020) 127439, https://doi.org/10.1016/j.chemosphere.2020.127439.
[12] J. You, J. Li, H. Zhang, M. Luo, B. Xing, Y. Ren, Y. Liu, Removal of Bisphenol A via peroxymonosulfate activation over graphite carbon nitride supported NiCx nanoclusters catalyst : synergistic oxidation of high-valent nickel-oxo species and singlet oxygen, J. Hazard Mater. 445 (2023) 130440, https://doi.org/10.1016/j.jhazmat.2022.130440.

[13] Science of the Total Environment W. Fan, G. Sun, Q. Wang, F. Yang, Y. Gao, M. Yang, Identifying the critical activated carbon properties affecting the adsorption of ef fl uent organic matter from bio-treated coking wastewater, Sci. Total Environ. 871 (2023) 161968, https://doi.org/10.1016/j.scitotenv.2023.161968.
[14] Journal of Water Process Engineering T. Ahmad, M. Saood, J. Georgin, D.S.P. Franco, S. Khan, L. Meili, N. Ullah, Development of a new hyper crosslinked resin based on polyamine-isocyanurate for the efficient removal of endocrine disruptor bisphenol-A from water, J. Water Process Eng. 53 (2023) 103623, https://doi.org/10.1016/j.jwpe.2023.103623.
[15] A.C. Arampatzidou, E.A. Deliyanni, Journal of Colloid and Interface Science Comparison of activation media and pyrolysis temperature for activated carbons development by pyrolysis of potato peels for effective adsorption of endocrine disruptor bisphenol-A, J. Colloid Interface Sci. 466 (2016) 101–112, https://doi.org/10.1016/j.jcis.2015.12.003.
[16] Journal of Water Process Engineering U.A. Qureshi, B.H. Hameed, M.J. Ahmed, Adsorption of endocrine disrupting compounds and other emerging contaminants using lignocellulosic biomass-derived porous carbons : a review, J. Water Process Eng. 38 (2020) 101380, https://doi.org/10.1016/j.jwpe.2020.101380.
[17] P.C. Bhomick, A. Supong, M. Baruah, C. Pongener, D. Sinha, Pine Cone biomass as an efficient precursor for the synthesis of activated biocarbon for adsorption of anionic dye from aqueous solution: isotherm, kinetic, thermodynamic and regeneration studies, Sustain. Chem. Pharm. 10 (2018) 41–49, https://doi.org/10.1016/j.scp.2018.09.001.
[18] B. Qiu, Q. Shao, J. Shi, C. Yang, H. Chu, Application of biochar for the adsorption of organic pollutants from wastewater : modification strategies , mechanisms and challenges, Separ. Purif. Technol. 300 (2022) 121925, https://doi.org/10.1016/j.seppur.2022.121925.
[19] B. Enyojo, A. Oluwasogo, U. Pal, Agro-waste based adsorbents as sustainable materials for effective adsorption of Bisphenol A from the environment : a review, J. Clean. Prod. 388 (2023) 135819, https://doi.org/10.1016/j.jclepro.2022.135819.
[20] Journal of Environmental Chemical Engineering S. Majumder, P. Sharma, S. Pratap, A. Kumar, P. Kumar, C. Xia, S. Sharma, R. Ganguly, S. Shiung, H. Kim, Engineered biochar for the effective sorption and remediation of emerging pollutants in the environment, J. Environ. Chem. Eng. 11 (2023) 109590, https://doi.org/10.1016/j.jece.2023.109590.
[21] A. Othmani, J. John, H. Rajendran, A. Mansouri, Biochar and activated carbon derivatives of lignocellulosic fibers towards adsorptive removal of pollutants from aqueous systems : Critical study and future insight, 274, 2021, https://doi.org/10.1016/j.seppur.2021.119062.
[22] W. Shi, H. Wang, J. Yan, L. Shan, G. Quan, X. Pan, Wheat straw derived biochar with hierarchically porous structure for Bisphenol A removal : preparation , characterisation, and adsorption properties, Separ. Purif. Technol. 289 (2022) 120796, https://doi.org/10.1016/j.seppur.2022.120796.
[23] Ecotoxicology and Environmental Safety C. Earn, S. Ibrahim, Y. Yoon, M. Jang, Removal of lead and bisphenol A using magnesium silicate impregnated palm-shell waste powdered activated carbon : comparative studies on single and binary pollutant adsorption, Ecotoxicol. Environ. Saf. 148 (2018) 142–151, https://doi.org/10.1016/j.ecoenv.2017.10.025.
[24] H. Laksaci, B. Belhamdi, O. Khelifi, A. Khelifi, Elimination of amoxicillin by adsorption on coffee waste based activated carbon, J. Mol. Struct. 1274 (2023) 134500, https://doi.org/10.1016/j.molstruc.2022.134500.
[25] Journal of environmental chemical engineering A. Ahsan, T. Islam, C. Hernandez, H. Kim, Y. Lin, M.L. Curry, J. Gardea-torresdey, J.C. Noveron, Adsorptive removal of sulfamethoxazole and bisphenol A from contaminated water using functionalized carbonaceous material derived from tea Leaves, J. Environ. Chem. Eng. 6 (2018) 4215–4225, https://doi.org/10.1016/j.jece.2018.06.022.
[26] X. Fang, Y. Wu, L. Xu, L. Gan, Fast removal of bisphenol A by coconut shell biochar incorporated α -MnO 2 composites via peroxymonosulfate activation, J. Water Process Eng. 49 (2022) 103071, https://doi.org/10.1016/j.jwpe.2022.103071.
[27] S. Sharma, S.L. Ezung, A. Supong, M. Baruah, S. Kumar, R.S. Umdor, D. Sinha, Activated carbon adsorbent derived from waste biomass , “ Croton caudatus ” for efficient removal of 2-chlorophenol from aqueous solution : kinetics , isotherm , thermodynamics and DFT simulation, Chem. Eng. Res. Des. 190 (2023) 777–792, https://doi.org/10.1016/j.cherd.2023.01.002.
[28] A. Chandrasekaran, C. Patra, S. Narayanasamy, Adsorptive removal of Cipro fl oxacin and Amoxicillin from single and binary aqueous systems using acid-activated carbon from Prosopis juli fl ora, Environ. Res. 188 (2020) 109825, https://doi.org/10.1016/j.envres.2020.109825.
[29] X. Lei, M. Wang, Y. Lai, L. Hu, H. Wang, Z. Fang, J. Li, J. Fang, Nitrogen-doped micropore-dominant carbon derived from waste pine cone as a promising metal-free electrocatalyst for aqueous zinc/air batteries, J. Power Sources 365 (2017) 76–82, https://doi.org/10.1016/j.jpowsour.2017.08.084.
[30] Bioresource Technology S. Dawood, T.K. Sen, C. Phan, Synthesis and characterisation of slow pyrolysis pine cone bio-char in the removal of organic and inorganic pollutants from aqueous solution by adsorption : kinetic , equilibrium , mechanism and thermodynamic, Bioresour. Technol. 246 (2017) 76–81, https://doi.org/10.1016/j.biortech.2017.07.019.
[31] S.A. Mirzaee, B. Bayati, M.R. Valizadeh, H.T. Gomes, Z. Noorimotlagh, Adsorption of diclofenac on mesoporous activated carbons: physical and chemical activation, modeling with genetic programming and molecular dynamic simulation, Chem. Eng. Res. Des. 167 (2021) 116–128, https://doi.org/10.1016/j.cherd.2020.12.025.
[32] F. Mbarki, T. Selmi, A. Kesraoui, M. Seffen, Low-cost activated carbon preparation from Corn stigmata fibers chemically activated using H3PO4, ZnCl2 and KOH: study of methylene blue adsorption, stochastic isotherm and fractal kinetic, Ind. Crop. Prod. 178 (2022) 114546, https://doi.org/10.1016/j.indcrop.2022.114546.
[33] A.S. Mestre, R.M.C. Viegas, E. Mesquita, M.J. Rosa, A.P. Carvalho, Engineered pine nut shell derived activated carbons for improved removal of recalcitrant pharmaceuticals in urban wastewater treatment, J. Hazard Mater. (2022) 129319, https://doi.org/10.1016/j.jhazmat.2022.129319.
[34] S. Valizadeh, H. Younesi, N. Bahramifar, Preparation and characterisation of activated carbon from the cones of Iranian pine trees (Pinus eldarica) by chemical activation with H3PO4 and its application for removal of sodium dodecylbenzene sulfonate removal from aqueous solution, Water Conserv. Sci. Eng. 3 (2018) 253–265, https://doi.org/10.1007/s41101-018-0055-5.
[35] G. Duman, Y. Onal, C. Okutucu, S. Onenc, J. Yanik, Production of activated carbon from pine cone and evaluation of its physical, chemical, and adsorption properties, Energy Fuel. 23 (2009) 2197–2204, https://doi.org/10.1021/ef800510m.
[36] J. Carlos, P. Hu, Activated carbons obtained from agro-industrial waste : textural analysis and adsorption environmental pollutants. https://doi.org/10.1007/s10450-015-9728-y, 2015.
[37] Y. Xue, Y. Guo, X. Zhang, M. Kamali, T.M. Aminabhavi, L. Appels, R. Dewil, Efficient adsorptive removal of ciprofloxacin and carbamazepine using modified pinewood biochar – a kinetic , mechanistic study, Chem. Eng. J. 450 (2022) 137896, https://doi.org/10.1016/j.cej.2022.137896.
[38] N.A.S. Mohammed, R.A. Abu-zurayk, I. Hamadneh, A.H. Al-dujaili, Phenol adsorption on biochar prepared from the pine fruit shells : equilibrium , kinetic and thermodynamics studies, J. Environ. Manag. 226 (2018) 377–385, https://doi.org/10.1016/j.jenvman.2018.08.033.
[39] H. Henrique, C. De Lima, M. Eug, M.P. Mois, V. Janeiro, P. Augusto, M. Rog, A. Wellington, Enhanced removal of bisphenol A using pine-fruit shell-derived hydrochars : Adsorption mechanisms and reusability, 416, 2021, https://doi.org/10.1016/j.jhazmat.2021.126167.
[40] K.K. Kishibayev, J. Serafin, R.R. Tokpayev, T.N. Khavaza, A.A. Atchabarova, Physical and Chemical properties of activated carbon synthesised from plant wastes and shungite for CO 2 capture, J. Environ. Chem. Eng. 9 (2021), https://doi.org/10.1016/j.jece.2021.106798.
[41] Journal of Environmental Chemical Engineering S. Sharafinia, A. Rashidi, M.D. Esrafili, Optimised adsorption of volatile organic compounds on the activated carbon prepared from mesquite grain : a combined experimental and computational study, J. Environ. Chem. Eng. 10 (2022) 108528, https://doi.org/10.1016/j.jece.2022.108528.
[42] H. Tounsadi, A. Khalidi, A. Machrouhi, M. Farnane, R. Elmoubarki, A. Elhalil, M. Sadiq, N. Barka, Highly efficient activated carbon from Glebionis coronaria L. biomass: optimisation of preparation conditions and heavy metals removal using experimental design approach, J. Environ. Chem. Eng. 4 (2016) 4549–4564, https://doi.org/10.1016/j.jece.2016.10.020.
[43] Y. Zhang, L. Liu, P. Zhang, J. Wang, M. Xu, Q. Deng, Z. Zeng, Ultra-high surface area and nitrogen-rich porous carbons prepared by a low- temperature activation method with superior gas selective adsorption and outstanding supercapacitance performance, Chem. Eng. J. 355 (2019) 309–319, https://doi.org/10.1016/j.cej.2018.08.169.
[44] C. Duan, M. Meng, H. Huang, H. Wang, Q. Zhang, Performance and characterisation of bamboo-based activated carbon prepared by boric acid activation, Mater. Chem. Phys. 295 (2023) 127130, https://doi.org/10.1016/j.matchemphys.2022.127130.

[45] G.V. Nunell, M.E. Fernandez, P.R. Bonelli, A.L. Cukierman, Nitrate uptake improvement by modified activated carbons developed from two species of pine cones, J. Colloid Interface Sci. 440 (2015) 102–108, https://doi.org/10.1016/j.jcis.2014.10.058.
[46] L. Nielsen, M.J. Biggs, W. Skinner, T.J. Bandosz, The effects of activated carbon surface features on the reactive adsorption of carbamazepine and sulfamethoxazole, Carbon 80 (2014) 419–432, https://doi.org/10.1016/j.carbon.2014.08.081.
[47] M. Chaker, M. Sillanpää, Optimising the removal of pharmaceutical drugs Carbamazepine and Dorzolamide from aqueous solutions using mesoporous activated carbons and multi-walled carbon nanotubes, J. Mol. Liq. 238 (2017) 379–388, https://doi.org/10.1016/j.molliq.2017.05.028.
[48] Z.H. Deng, N. Li, H.L. Jiang, J.M. Lin, R.S. Zhao, Pretreatment techniques and analytical methods for phenolic endocrine disrupting chemicals in food and environmental samples, TrAC, Trends Anal. Chem. 119 (2019), https://doi.org/10.1016/j.trac.2019.07.003.
[49] Z. Fang, Y. Hu, Y. Qin, J. Cheng, A novel magnesium ascorbyl phosphate graphene-based monolith and its superior adsorption capability for bisphenol A, Chem. Eng. J. (2017), https://doi.org/10.1016/j.cej.2017.10.067.
[50] F. Marrakchi, M. Wei, B. Cao, C. Yuan, H. Chen, S. Wang, Copyrolysis of microalga Chlorella sp. and alkali lignin with potassium carbonate impregnation for synergistic Bisphenol A plasticiser adsorption, Int. J. Biol. Macromol. 228 (2023) 808–815, https://doi.org/10.1016/j.ijbiomac.2022.12.207.
[51] Chemosphere R. Chandrasekar, H.K. Rajendran, V.P. V, S. Narayanasamy, Valorization of sawdust by mineral acid assisted hydrothermal carbonisation for the adsorptive removal of bisphenol A : a greener approach, Chemosphere 303 (2022) 135171, https://doi.org/10.1016/j.chemosphere.2022.135171.
[52] B.S. Rathi, P.S. Kumar, Application of adsorption process for effective removal of emerging contaminants from water and wastewater, Environ. Pollut. 280 (2021) 116995, https://doi.org/10.1016/j.envpol.2021.116995.
[53] İ. Tosun, Ammonium removal from aqueous solutions by clinoptilolite, in: Determination of Isotherm and Thermodynamic Parameters and Comparison of Kinetics by the Double Exponential Model and Conventional Kinetic Models, 2012, pp. 970–984, https://doi.org/10.3390/ijerph9030970.
[54] J. Alca, Microporous and Mesoporous Materials Preparation of Binderless Activated Carbon Monoliths from Cocoa Bean Husk, vol. 243, 2017, pp. 28–38, https://doi.org/10.1016/j.micromeso.2017.02.015.
[55] Chemosphere R. Natarajan, K. Banerjee, P. Senthil, T. Somanna, D. Tannani, V. Arvind, R. Immanuel, D.N. Vo, K. Saikia, V. Kumar, Performance study on adsorptive removal of acetaminophen from wastewater using silica microspheres : kinetic and isotherm studies, Chemosphere 272 (2021) 129896, https://doi.org/10.1016/j.chemosphere.2021.129896.
[56] A.B. Hernández-Abreu, S. Álvarez-Torrellas, V.I. Águeda, M. Larriba, J.A. Delgado, P.A. Calvo, J. García, Enhanced removal of the endocrine disruptor compound Bisphenol A by adsorption onto green-carbon materials. Effect of real effluents on the adsorption process, J. Environ. Manag. 266 (2020), https://doi.org/10.1016/j.jenvman.2020.110604.
[57] Y. Tang, Y. Li, L. Zhan, D. Wu, S. Zhang, R. Pang, B. Xie, Removal of emerging contaminants (bisphenol A and antibiotics) from kitchen wastewater by alkali-modi fi ed biochar, Sci. Total Environ. 805 (2022), https://doi.org/10.1016/j.scitotenv.2021.150158.
[58] Journal of environmental chemical engineering R. Acosta, D. Nabarlatz, J. Jagiello, P. Gadonneix, A. Celzard, Adsorption of bisphenol A on KOH-activated tyre pyrolysis char, J. Environ. Chem. Eng. 6 (2018) 823–833, https://doi.org/10.1016/j.jece.2018.01.002.
[59] A. Islam, M.J. Ahmed, W.A. Khanday, M. Asif, B.H. Hameed, Mesoporous activated carbon prepared from NaOH activation of rattan (Lacosperma secundiflorum) hydrochar for methylene blue removal, Ecotoxicol. Environ. Saf. 138 (2017) 279–285, https://doi.org/10.1016/j.ecoenv.2017.01.010.
[60] Science of the Total Environment P. Ndagijimana, X. Liu, Z. Li, G. Yu, Y. Wang, Optimised synthesis of a core-shell structure activated carbon and its adsorption performance for Bisphenol A, Sci. Total Environ. 689 (2019) 457–468, https://doi.org/10.1016/j.scitotenv.2019.06.235.
[61] R. Wirasnita, T. Hadibarata, Removal of bisphenol A from aqueous solution by activated carbon derived from oil palm empty fruit bunch. https://doi.org/10.1007/s11270-014-2148-x, 2014.
[62] Q. Xu, X. Liu, D. Lai, Z. Xing, P. Ndagijimana, One-step synthesis of nanoscale zero-valent iron modified hydrophobic mesoporous activated carbon for efficient removal of bulky organic pollutants, J. Clean. Prod. 356 (2022) 131854, https://doi.org/10.1016/j.jclepro.2022.131854.
[63] L.B. Silva, F. Schimidt, Utilization of the Corncob Agro-Industrial Residue as a Potential Adsorbent in the Biosorption of Bisphenol-A, vol. 32, 2021, pp. 1396–1404.
[64] A. Supong, P.C. Bhomick, M. Baruah, C. Pongener, U.B. Sinha, D. Sinha, Adsorptive removal of Bisphenol A by biomass activated carbon and insights into the adsorption mechanism through density functional theory calculations, Sustain. Chem. Pharm. 13 (2019) 100159, https://doi.org/10.1016/j.scp.2019.100159.
[65] Journal of Environmental Chemical Engineering P.S. Pamidimukkala, H. Soni, Efficient removal of organic pollutants with activated carbon derived from palm shell : spectroscopic characterisation and experimental optimisation, J. Environ. Chem. Eng. 6 (2018) 3135–3149, https://doi.org/10.1016/j.jece.2018.04.013.
[66] A.C.F. Alves, R.V.P. Antero, S.B. de Oliveira, S.A. Ojala, P.S. Scalize, Activated carbon produced from waste coffee grounds for an effective removal of bisphenol-A in aqueous medium, Environ. Sci. Pollut. Control Ser. 26 (2019) 24850–24862, https://doi.org/10.1007/s11356-019-05717-7.
[67] P. Taylor, K. Chang, J. Hsieh, B. Ou, M. Chang, W. Hseih, K. Chang, J. Hsieh, B. Ou, M. Chang, Separation science and technology adsorption studies on the removal of an endocrine- disrupting compound (bisphenol A) using activated carbon from rice straw agricultural waste adsorption studies on the removal of an endocrine-disrupting compound (bisp, 37–41. https://doi.org/10.1080/01496395.2011.647212, 2012.
[68] G. Jaria, V. Calisto, V.I. Esteves, M. Otero, Overview of relevant economic and environmental aspects of waste-based activated carbons aimed at adsorptive water treatments, J. Clean. Prod. 344 (2022) 1–15, https://doi.org/10.1016/j.jclepro.2022.130984.